

Large-Pore Mesoporous Organosilicas Functionalized with *trans*-(1*R*,2*R*)-Diaminocyclohexane: Synthesis, Postmodification, and Catalysis

Dongmei Jiang, Jinsuo Gao, Qihua Yang,* Jie Yang, and Can Li*

State Key Laboratory of Catalysis, Dalian Institute of Chemical Physics, Chinese Academy of Sciences, 457 Zhongshan Road, Dalian 116023, China

Received June 7, 2006. Revised Manuscript Received September 15, 2006

Large-pore mesoporous ethane-silicas functionalized with *trans*-(1*R*,2*R*)-diaminocyclohexane were synthesized in an acidic medium by one-step co-condensation of 1,2-bis(trimethoxysilyl)ethane and *N*-[(trimethoxysilyl)benzyl]-(-)-(1*R*,2*R*)-diaminocyclohexane using triblock copolymer P123 as template. The postmodification of *trans*-(1*R*,2*R*)-diaminocyclohexane in the pore of the mesoporous ethane-silicas was further demonstrated by reaction with *p*-toluenesulfonyl chloride. The modified material (complexed with [RhCp*Cl₂]₂) exhibits much higher conversion and ee [53% conversion with 68% ee (R)] than the original material [18% conversion with 38% ee (S)] for the asymmetric transfer hydrogenation of acetophenone under air atmosphere in HCOONa–H₂O. Various aromatic ketones can be converted to the corresponding chiral alcohol with moderate to good enantioselectivities [18–81% ee (R)]. The co-condensation method associated with the postmodification method is one of the alternatives for the synthesis of mesoporous materials containing new functionalities.

1. Introduction

Mesoporous silicas functionalized with organic moiety are attractive in the fields of catalysis, adsorption, separation, drug delivery, and so on.^{1–3} In general, introducing organic moiety into mesoporous materials can be achieved either by a grafting (a postsynthesis method) or a co-condensation method (a direct synthesis method).⁴ The grafting method, which has been popularly used for introducing organic groups into the mesoporous silicas, would likely graft organic groups mainly on the external surface of the mesoporous particles or near the pore mouth because of the mass transfer. Compared with grafting techniques, the co-condensation method would likely result in mesoporous materials with a more uniform distribution of organic groups and a higher loading of organic groups without closing the mesopores. However, the direct synthesis method will often meet the challenge that is how to keep the highly ordered mesostructure of materials and incorporate enough organic functionalized group (especially large organic group) simultaneously. One of the alternatives for obtaining ordered mesoporous material with large functional group is the postmodification of the functionalized mesoporous materials through further chemical reaction. The postmodification method can avoid the tedious process for the design and synthesis of new organosilane precursors and reduce the difficulty in the

synthesis of highly ordered mesoporous material containing large functional group.

Recently, the periodic mesoporous organosilicas (PMOs) with organic groups bridged in the framework have been reported.^{4,5} More interestingly, the chiral moiety was incorporated into the framework of MCM-41 type mesoporous silicas by co-condensation method under basic medium using cationic surfactants.^{6–9} The pore diameter of the above materials is usually <4 nm, which limits their application in the heterogeneous catalysis involving large substrates. Analogous materials with large pore size and thick pore wall, such as SBA-15 type materials, are desirable and interesting.¹⁰ There has been no report, until now, about the synthesis of large-pore mesoporous materials functionalized with chiral moieties by co-condensation method under acidic conditions.

trans-(1,2)-Diaminocyclohexane (DACH) and its derivatives are among the most often used chiral ligands.¹¹ Recently, our group reported the synthesis and catalytic properties of MCM-41 type mesoporous ethane-silicas with

* Authors to whom correspondence should be addressed. Fax: +86-411-84694447. Q. Yang: e-mail, yangqh@dicp.ac.cn; web address, http://hmm.dicp.ac.cn. C. Li: e-mail, canli@dicp.ac.cn; web address, http://canli.dicp.ac.cn.

(1) Thomas, B. *Curr. Opin. Solid State Mater. Sci.* **1999**, 4, 85.

(2) Li, C. *Catal. Rev.-Sci. Eng.* **2004**, 46, 419.

(3) Corma, A. *Chem. Rev.* **1997**, 97, 2373.

(4) Hoffmann, F.; Cornelius, M.; Morell, J.; Fröba, M. *Angew. Chem., Int. Ed.* **2006**, 45, 3216.

(5) (a) Ingagaki, S.; Guan, S.; Fukushima, Y.; Ohsuna, T.; Terasaki, O. *J. Am. Chem. Soc.* **1999**, 121, 9611. (b) Melde, B. J.; Hollan, B. T.; Blanford, C.F.; Stein, A. *Chem. Mater.* **1999**, 11, 3302. (c) Asefa, T.; MacLachlan, M. J.; Coombs, N.; Ozin, G. A. *Nature* **1999**, 402, 867.

(6) Baleião, C.; Gigante, B.; Das, D.; Álvaro, M.; García, H.; Corma, A. *Chem. Commun.* **2003**, 1860.

(7) Álvaro, M.; Benitez, M.; Das, D.; Ferrer, B.; García, H. *Chem. Mater.* **2004**, 16, 2222.

(8) Baleião, C.; Gigante, B.; Das, D.; Álvaro, M.; García, H.; Corma, A. *J. Catal.* **2004**, 223, 106.

(9) Jiang, D. M.; Yang, Q. H.; Wang, H.; Zhu, G. R.; Yang, J.; Li, C. J. *Catal.* **2006**, 239, 65.

(10) (a) Zhao, D.; Feng, J.; Huo, Q.; Melosh, N.; Fredrickson, G. H.; Chmelka, B. F.; Stucky, G. D. *Science* **1998**, 279, 548. (b) Zhao, D.; Huo, Q.; Feng, J.; Chmelka, B. F.; Stucky, G. D. *J. Am. Chem. Soc.* **1998**, 120, 6024.

(11) Bennani, Y. L.; Hanessian, S. *Chem. Rev.* **1997**, 97, 3161.

DACH in the pore.¹² It is interesting that the presence of ethane group in the framework enhances the catalytic activity of the resulting catalysts compared to the pure mesoporous silica counterparts in the asymmetric transfer hydrogenation (ATH) of acetophenone. However, only moderate ee value (19–23%) was obtained because of the inherent low chiral inductivity of DACH. Very recently, Xiao and co-workers reported that, DACH derivative, (1*R*,2*R*)-*N*-(*p*-toluenesulfonyl)-1,2-cyclohexanediamine-Rh, is an efficient catalyst in the ATH of aromatic ketones by HCOONa in water under air atmosphere.¹³ Their studies illustrate a possibility that the chiral inductivity of DACH protruding into the pore of the mesoporous materials could also be enhanced by further chemical modification. The chiral solids with high chiral inductivity are interesting because of their potential application in asymmetric catalysis and chiral separation.

In this paper, we synthesized large-pore mesoporous ethane-silicas functionalized with DACH by co-condensation method under an acidic medium using P123 as surfactant for the first time. The ethane moiety bridging in the framework may enhance the catalytic activity of the resulting catalysts for the ATH of acetophenone. The DACH protruding in the mesopore was further modified through reaction with *p*-toluenesulfonyl chloride. The chiral inductivity of the modified mesoporous material is greatly enhanced in the ATH of acetophenone using HCOONa–H₂O under air atmosphere.

2. Experimental Section

2.1. Chemicals. The solvents are of analytical quality and dried by standard methods. Other materials are analytical grade and used as purchased without further purification. Triblock PEO–PPO–PEO copolymer P123 [HO(CH₂CH₂O)₂₀(CH₂CH(CH₃)O)₇₀(CH₂CH₂O)₂₀H] and 1,2-bis(trimethoxysilyl)ethane (BTME) were purchased from Sigma-Aldrich Company Ltd. 4-(Chloromethyl)phenyltrimethoxysilane was purchased from Gelest Inc. *trans*-(1*R*,2*R*)-Diaminocyclohexane was obtained by resolution of a commercially available mixture of *cis*- and *trans*-diaminocyclohexane (30/70) according to the literature.¹⁴ *N*-[4-(trimethoxysilyl)benzyl]-(-)-(1*R*,2*R*)-diaminocyclohexane (**M**_{benzyl}) was prepared according to ref 9. Dichloro(pentamethylcyclopentadienyl)rhodium(III) dimer ([RhCp*Cl₂)₂) and chloro(1,3-cyclooctadiene)rhodium(I) dimer ([Rh(cod)Cl]₂) were purchased from Strem.

2.2. Synthetic Procedures. **2.2.1. Synthesis of Mesoporous Organosilicas with *trans*-(1*R*,2*R*)-Diaminocyclohexane in the Channel (SBA_{benzyl}-*n*-N).** For a typical synthesis, P123 (1.1 g) and KCl (6.98 g) were dissolved in a solution containing HCl (33 g, 2 M) and H₂O (7.5 g) at 40 °C under vigorous stirring. A mixture (8.62 mmol) of BTME and **M**_{benzyl} was added to the above solution. The reaction mixture was stirred at 40 °C for 24 h and aged at 100 °C under static conditions for 24 h. The solid product was recovered by filtration. The surfactant was extracted twice by refluxing 1 g of as-synthesized material in 300 mL of ethanol for 24 h. The product containing protonated *trans*-(1*R*,2*R*)-diaminocyclohexane (1 g) was stirred in 50 mL of tetramethylammonium hydroxide methanol solution (0.2 M) for 1 h at room temperature to obtain

the free base. After filtration, the powder product was washed with copious amounts of water and ethanol and dried under vacuum at 60 °C. The materials were denoted as SBA_{benzyl}-*n*-N, while *n* (*n* = 0, 10, 20, 30) is the molar percent of **M**_{benzyl}/(**M**_{benzyl} + BTME).

2.2.2. Synthesis of Mesoporous Silicas with *trans*-(1*R*,2*R*)-Diaminocyclohexane in the Channel (SSBA_{benzyl}-10-N). For comparison, mesoporous silica containing *trans*-(1*R*,2*R*)-diaminocyclohexane (SSBA_{benzyl}-10-N) was also synthesized. P123 (4 g) and NaCl (11 g) were dissolved in a solution containing HCl (125 g, 2 M) with stirring at room temperature. After TEOS (7.06 g) was added, the resultant solution was hydrolyzed at 40 °C for 2 h. Then **M**_{benzyl} (1.22 g) dissolved in EtOH (0.4 g) was slowly added into the above solution. The resulting mixture was stirred at 40 °C for 24 h and then aged at 100 °C under static conditions for 24 h. The solid product was recovered by filtration. The extraction of surfactant and release of protonated *trans*-(1*R*,2*R*)-diaminocyclohexane in the material is similar to those of SBA_{benzyl}-*n*-N. The resulting material was denoted as SSBA_{benzyl}-10-N, while 10 is the molar percent of **M**_{benzyl}/(**M**_{benzyl} + TEOS).

2.2.3. Postmodification of SBA_{benzyl}-30-N and SSBA_{benzyl}-10-N with *p*-Toluenesulfonyl Chloride. In a round-bottomed flask (50 mL) equipped with a reflux condenser, 0.10 g of SBA_{benzyl}-30-N or SSBA_{benzyl}-10-N was dried at 120 °C under vacuum for 4 h. After it was cooled to room temperature, freshly distilled toluene (10 mL) and Et₃N were added under argon atmosphere. *p*-Toluenesulfonyl chloride in freshly distilled toluene (10 mL) was dropwise added to the above solution (the molar ratio of *trans*-(1*R*,2*R*)-diaminocyclohexane:*p*-toluenesulfonyl chloride:Et₃N = 1:10:10). The mixture was magnetically stirred for 15 h at 70 °C under argon atmosphere. After filtration, the solid product was thoroughly washed with dichloromethane and dried under vacuum at 60 °C overnight. The modified samples were denoted as SBA_{benzyl}-30-NTs and SSBA_{benzyl}-10-NTs, respectively. The S and N elemental analyses show that the molar ratio of S/N in the SBA_{benzyl}-30-NTs is about 1:1.

2.2.4. Complexing SBA_{benzyl}-*n*-N and SSBA_{benzyl}-10-N with [Rh(cod)Cl]₂. [Rh(cod)Cl]₂ in 15 mL of dry ethanol was added to a Schlenk tube containing 0.2 g of SBA_{benzyl}-*n*-N or SSBA_{benzyl}-10-N. The molar ratio of *trans*-(1*R*,2*R*)-diaminocyclohexane:[Rh(cod)Cl]₂ is 1:0.75. After the mixture was stirred for 48 h under argon atmosphere at room temperature, the yellow powder product was filtered and washed with freshly distilled THF to eliminate the free rhodium complex and then dried under vacuum. The catalysts were denoted as SBA_{benzyl}-*n*-NRh (*n* = 10, 20, 30) and SSBA_{benzyl}-10-NRh, respectively.

2.2.5. Complexing SBA_{benzyl}-30-N, SBA_{benzyl}-30-NTs, and SSBA_{benzyl}-10-NTs with [RhCp*Cl₂]₂. The complexing method was the same as that of SBA_{benzyl}-*n*-NRh, except that [RhCp*Cl₂]₂ was used instead of [Rh(cod)Cl]₂ and 2 equiv of Et₃N was introduced to eliminate HCl produced during the reaction. The catalysts were denoted as SBA_{benzyl}-30-NRhCp, SBA_{benzyl}-30-NTsRhCp, and SSBA_{benzyl}-10-NTsRhCp.

2.3. Characterization. X-ray powder diffraction (XRD) patterns were recorded on a Rigaku D/Max 3400 powder diffraction system using Cu Kα radiation (40 kV and 30 mA). Transmission electron microscopy (TEM) measurements were recorded on a JEM-2010 at an acceleration voltage of 120 kV. Nitrogen sorption isotherms were measured at 77 K on an ASAP 2000 system in static measurement mode. The sample was degassed at 373 K prior to the measurement. Pore diameter was calculated from the adsorption branch of the isotherm using the Barrett–Joyner–Halenda (BJH) method. Solid-state ¹³C (100.5 MHz) and ²⁹Si (79.4 MHz) CP-MAS NMR spectra were obtained on a Bruker DRX-400 spectrometer with the following experimental parameters: for ¹³C CP-

(12) Jiang, D. M.; Yang, Q. H.; Yang, J.; Zhang, L.; Zhu, G. R.; Su, W. G.; Li, C. *Chem. Mater.* **2005**, *17*, 6154.

(13) Wu, X. F.; Vinci, D.; Ikariya, T.; Xiao, J. L. *Chem. Commun.* **2005**, 4447.

(14) Jay, F. L.; Eric, N. J. *J. Org. Chem.* **1994**, *59*, 1939.

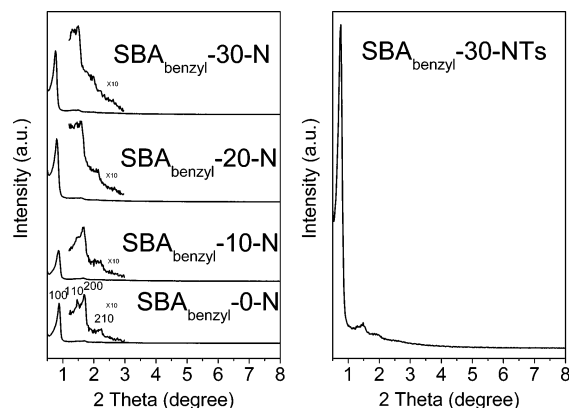


Figure 1. Powder XRD patterns of SBA_{benzyl}-*n*-N [*n* is the molar percent of M_{benzyl}/(M_{benzyl} + BTME)] and SBA_{benzyl}-30-NTs [the material prepared by postmodification of SBA_{benzyl}-30-N with *p*-toluenesulfonyl chloride].

MAS NMR experiments, 8 kHz spin rate, 3 s pulse delay, 4 min contact time, 1000 scans; for ²⁹Si CP-MAS NMR experiments, 8 kHz spin rate, 3 s pulse delay, 10 min contact time, 1000 scans. Tetramethylsilane was used as a reference. N and Rh elemental analyses were respectively performed on an Elementar Vario EL III (Germany) and a Plasma-spec-II (Leeman. Labs. U.S.A.). Infrared spectra were recorded on a Thermo Nicolet Nexus 470 FT-IR spectrometer. Self-supporting wafer was loaded into an IR cell with CaF₂ windows. Before measurement, the wafer was degassed at 150 °C for 2 h under vacuum (10⁻² Pa). Diffuse reflectance UV–vis spectra were collected on a JASCO V-550 UV–vis spectrophotometer using BaSO₄ as a reference.

2.4. Catalytic Reaction. **2.4.1. Asymmetric Transfer Hydrogenation (ATH) of Acetophenone with Isopropanol as H-Donor.** The ATH of acetophenone was carried out under argon atmosphere. The catalyst (7.36 μmol of Rh) was vacuumed in a flask (50 mL) for 1 h at room temperature. The freshly distilled isopropanol (12 mL) and *i*-PrOK (0.1 mmol) were added. The suspension was stirred for 1 h at room temperature and ketone (2 mmol) was added with a syringe. The reaction mixture was stirred at 83 ± 2 °C for 3 h under argon atmosphere. The catalytic activity and enantiomeric excess were measured on an Agilent 6890 gas chromatograph equipped with a flame ionization detector and an HP-Chiral 19091G-B213 capillary column (30 m × 0.32 mm × 0.25 μm).

2.4.2. Asymmetric Transfer Hydrogenation (ATH) of Aromatic Ketones with HCOONa as H-Donor. The reaction was performed under air atmosphere. The mixture containing catalyst (0.01 mmol of Rh), HCOONa (5 mmol), ketone (0.5 mmol), and distilled water (2 mL) was stirred for 10 h at 40 °C. After reaction, the products were extracted with Et₂O, dried with MgSO₄, and analyzed by an Agilent 6890 gas chromatograph equipped with a flame ionization detector and an HP-Chiral 19091G-B213 capillary column (30 m × 0.32 mm × 0.25 μm).

3. Results and Discussion

3.1. Structural Characterization. XRD patterns of SBA_{benzyl}-*n*-N are presented in Figure 1. The XRD pattern of SBA_{benzyl}-0-N (without chiral moiety) exhibits an intense *d*₁₀₀ diffraction peak along with three weak diffractions (*d*₁₁₀, *d*₂₀₀, *d*₂₁₀), showing that the material has highly ordered 2-D hexagonal mesostructure. SBA_{benzyl}-*n*-N (*n* = 10, 20, 30) shows a similar XRD pattern to that of SBA_{benzyl}-0-N. The XRD results indicate that the highly ordered mesoporous ethane-silicas with chiral moiety in the pore could be

Table 1. Physicochemical Parameters for the Mesoporous Materials Functionalized with *trans*-(1*R*,2*R*)-Diaminocyclohexane

| sample | <i>d</i> ₁₀₀ spacing (nm) | <i>S</i> _{BET} (m ² /g) | pore volume ^a (cm ³ /g) | pore diameter ^b (nm) | <i>a</i> ₀ ^c (nm) | wall thickness ^d (nm) |
|--------------------------------|--|--|---|---------------------------------------|--|--|
| SBA _{benzyl} -0-N | 10.1 | 725 | 0.71 | 7.5 | 11.7 | 4.2 |
| SBA _{benzyl} -10-N | 10.3 | 647 | 0.67 | 7.6 | 11.9 | 4.3 |
| SBA _{benzyl} -20-N | 11.0 | 566 | 0.64 | 7.4 | 12.7 | 5.3 |
| SBA _{benzyl} -30-N | 11.6 | 511 | 0.58 | 7.5 | 13.4 | 5.9 |
| SBA _{benzyl} -30-NTs | 11.6 | 282 | 0.42 | 6.9 | 13.4 | 6.5 |
| SSBA _{benzyl} -10-N | 8.2 | 543 | 0.67 | 6.0 | 9.5 | 3.5 |
| SSBA _{benzyl} -10-NTs | 8.1 | 474 | 0.63 | 5.6 | 9.4 | 3.8 |

^a Total pore volume calculated at *P*/*P*₀ = 0.99. ^b Calculated from adsorption isotherm. ^c *a*₀ is the lattice parameter. *a*₀ = 2*d*₁₀₀/√3. ^d Wall thickness = *a*₀ − pore diameter.

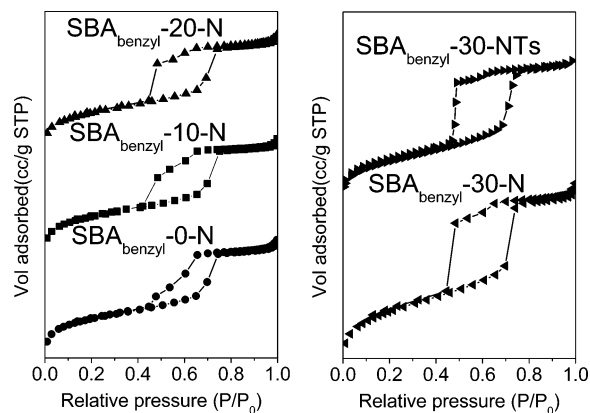


Figure 2. Nitrogen adsorption–desorption isotherms of SBA_{benzyl}-*n*-N [*n* is the molar percent of M_{benzyl}/(M_{benzyl} + BTME)] and SBA_{benzyl}-30-NTs [the material prepared by postmodification of SBA_{benzyl}-30-N with *p*-toluenesulfonyl chloride].

synthesized under current synthetic conditions. As the amount of M_{benzyl} in the initial gel mixture increases, the *d*₁₀₀ diffraction peak shifts to lower diffraction angle (Table 1). The expansion of the unit cell with M_{benzyl} concentration increasing may be proof of the fact that greater amounts of chiral moiety were incorporated in the material.

Nitrogen adsorption–desorption isotherms of SBA_{benzyl}-*n*-N (*n* = 0, 10, 20, 30) are displayed in Figure 2. SBA_{benzyl}-0-N exhibits a type IV sorption isotherm with H1 hysteresis loop according to IUPAC classification. It is to be noted that the desorption branch shows a slight tail extending toward a lower relative pressure of *P*/*P*₀ = 0.44. The sorption isotherms of SBA_{benzyl}-*n*-N (*n* = 10, 20, 30) are also of typical type IV. The substep desorptions at *P*/*P*₀ of 0.65 and the broadening of the hysteresis loops were observed for SBA_{benzyl}-*n*-N (*n* = 10, 20, 30). The results of N₂ sorption isotherms indicate the formation of plugs in the channel of SBA_{benzyl}-*n*-N (*n* = 0, 10, 20, 30). This phenomenon is rationalized based on the fact that an excess silica source (Si/P123 = 90–77) was added during the synthesis process, which is in the similar range (Si/P123 > 60) for the synthesis of SBA-15 with plugged mesopore.¹⁵ The hysteresis changes with M_{benzyl} concentration increasing can be explained by

- (15) (a) Van der Voort, P.; Ravikovitch, P. I.; de Jong, K. P.; Neimark, A. V.; Janssen, A. H.; Benjelloun, M.; Van Bavel, E.; Cool, P.; Weckhuysen, B. M.; Vansant, E. F. *Chem. Commun.* **2002**, 1010. (b) Van der Voort, P.; Ravikovitch, P. I.; de Jong, K. P.; Benjelloun, M.; Van Bavel, E.; Janssen, A. H.; Neimark, A. V.; Weckhuysen, B. M.; Vansant, E. F. *J. Phys. Chem. B* **2002**, 106, 5873.

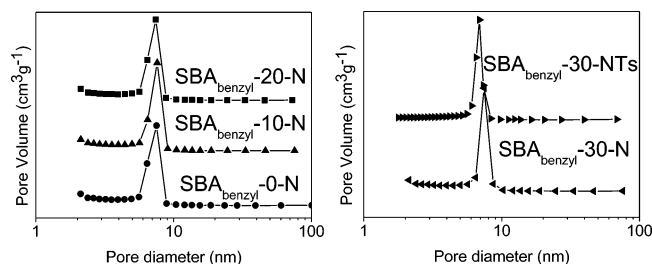


Figure 3. Pore size distributions of $\text{SBA}_{\text{benzyl}}-n\text{-N}$ calculated from the adsorption isotherms based BJH method [n is the molar percent of M_{benzyl} (M_{benzyl} + BTME)] and $\text{SBA}_{\text{benzyl}}-30\text{-NTs}$ [the material prepared by postmodification of $\text{SBA}_{\text{benzyl}}-30\text{-N}$ with *p*-toluenesulfonyl chloride].

the different hydrolysis and condensation rate between different silane precursors (M_{benzyl} and BTME).^{16,17}

The BET surface area and pore volume of $\text{SBA}_{\text{benzyl}}-n\text{-N}$ ($n = 0, 10, 20, 30$) decrease with increasing the concentration of M_{benzyl} in the initial gel mixture (Table 1). The opposite tendency was observed for the wall thickness (Table 1). The increased wall thickness may be due to the fact that greater amounts of chiral moiety are exposed on the surface of the pore channel. The pore size distribution of $\text{SBA}_{\text{benzyl}}-n\text{-N}$ ($n = 0, 10, 20, 30$) indicates the presence of uniform mesopore (~ 7.5 nm) (Figure 3 and Table 1). TEM images of $\text{SBA}_{\text{benzyl}}-n\text{-N}$ ($n = 10, 20, 30$) further confirm the hexagonal arrangement of the mesopore throughout the sample (Figure 4), which is consistent with the results of XRD and N_2 sorption isotherms.

$\text{SBA}_{\text{benzyl}}-30\text{-NTs}$, prepared by postmodification of $\text{SBA}_{\text{benzyl}}-30\text{-N}$ with *p*-toluenesulfonyl chloride, exhibits almost similar XRD pattern to that of $\text{SBA}_{\text{benzyl}}-30\text{-N}$ (Figure 1), suggesting that the mesostructure of $\text{SBA}_{\text{benzyl}}-30\text{-N}$ is robust enough to survive the rigorous postmodification process. The N_2 sorption isotherm of $\text{SBA}_{\text{benzyl}}-30\text{-NTs}$ is also of type IV with a wide H1 hysteresis loop (Figure 2), again demonstrating that the mesostructure of the material is maintained after modification. After modification, the decreasing of BET surface area, pore volume, and pore diameter is also observed (Table 1). The new chiral moiety, generated after reaction of *trans*-(1*R*,2*R*)-diaminocyclohexane with *p*-toluenesulfonyl chloride, is larger than the original chiral moiety. This can partly explain the decreasing of pore volume and pore diameter after modification.

$\text{SSBA}_{\text{benzyl}}-10\text{-N}$ was synthesized by co-condensation of TEOS and M_{benzyl} under acidic conditions. A high intensive d_{100} diffraction peak together with two higher angle peaks of d_{110} and d_{200} scatterings is observed in the XRD pattern of $\text{SSBA}_{\text{benzyl}}-10\text{-N}$ (Figure 5). The N_2 sorption isotherms further show that $\text{SSBA}_{\text{benzyl}}-10\text{-N}$ has well-ordered mesostructure with high BET surface area of $543 \text{ m}^2/\text{g}$ and narrow pore diameters of 6.0 nm (Table 1 and Figure 5). For $\text{SSBA}_{\text{benzyl}}-10\text{-NTs}$ prepared by further postmodification of $\text{SSBA}_{\text{benzyl}}-10\text{-N}$ using *p*-toluenesulfonyl chloride, XRD and N_2 sorption isotherms show the material still has well-ordered mesostructure with BET surface area of $474 \text{ m}^2/\text{g}$ and pore diameter of 5.6 nm.

3.2. Compositional Analysis. The FT-IR spectrum of $\text{SBA}_{\text{benzyl}}-30\text{-N}$ using a self-supporting wafer under vacuum is presented in Figure 6. The peaks at 1410 and 1271 cm^{-1} are attributed to the C–H deformation vibration of the bridged ethane group.¹⁸ The band at 1456 cm^{-1} is the characteristic C–H deformation vibration of cyclohexane and phenyl of M_{benzyl} . The broad bands at 3358 and 3303 cm^{-1} are ascribed to the asymmetric and symmetric N–H stretching vibrations, respectively.¹⁹ The N–H scissoring vibration at 1590 cm^{-1} is overwhelmed by the $\text{C}=\text{C}_{\text{aromatic}}$ stretching vibration at 1609 cm^{-1} .^{19–21} The C–H_{aromatic} stretchings are also clearly observed at 3073 and 3038 cm^{-1} .²² The disappearance of the C–H bending vibration of P123 at 1377 cm^{-1} indicates the almost complete removal of the surfactant using the EtOH extraction method.

The integrity of the organic group in $\text{SBA}_{\text{benzyl}}-30\text{-N}$ is further identified by solid-state NMR (Figure 7). The ^{13}C CP-MAS NMR spectrum of $\text{SBA}_{\text{benzyl}}-30\text{-N}$ displays signals corresponding to cyclic CH_2 in the range of 20.0 – 30.0 ppm.²³ The signals at 53.7 and 57.7 ppm can be assigned to NCH and NCH₂, respectively.²³ The existence of phenyl group is confirmed by the signals at 128.6 , 134.9 , and 141.4 ppm, among which the peak at 134.9 ppm is attributed to the carbon in M_{benzyl} connected to Si.^{9,24} The sharp signal at 5.4 ppm is ascribed to the ethane moiety bridged in the mesoporous framework.²⁵ In the ^{29}Si CP MAS NMR spectrum, three signals at -59.1 , -65.3 , and -80 ppm are observed. The signals at -59.1 and -65.3 ppm can be assigned to T² [$\text{SiC}(\text{OH})(\text{OSi})_2$] and T³ [$\text{SiC}(\text{OSi})_3$] for Si species bridged by ethane moiety, respectively. The signal at -80.4 ppm is T^{3'} [$\text{SiC}(\text{OSi})_3$] for Si species bonded with the phenyl in the chiral moiety.⁹ The absence of resonances assignable to SiO_4 species such as Q³ [$\text{Si}(\text{OH})(\text{OSi})_3$] and Q⁴ [$\text{Si}(\text{OSi})_4$] (from -90 to -120 ppm) confirms that the Si–C bond remains intact during synthesis and surfactant extraction.

The FT-IR spectrum of $\text{SBA}_{\text{benzyl}}-30\text{-NTs}$ is similar to that of $\text{SBA}_{\text{benzyl}}-30\text{-N}$ (Figure 6). However, the double peaks at 3303 and 3353 cm^{-1} corresponding to the primary amine of M_{benzyl} disappear. Instead, a weak broad vibration appears in the range of 3360 – 3300 cm^{-1} , demonstrating that one H of the NH_2 in M_{benzyl} was reacted with *p*-toluenesulfonyl chloride during the postmodification process.²⁶ Moreover, a new peak at 1331 cm^{-1} , ascribed to the $\text{O}=\text{S}=\text{O}$ vibration

(16) Kruk, M.; Jaroniec, M.; Joo, S. H.; Ryoo, R. *J. Phys. Chem. B* **2003**, *107*, 2205.

(17) Bao, X. Y.; Li, X.; Zhao, X. S. *J. Phys. Chem. B* **2006**, *110*, 2656.

(18) Much, O.; Schellbach, C.; Fröba, M. *Chem. Commun.* **2001**, 2032.

(19) Socrates, G. *Infrared Characteristic Group Frequencies, Tables and Charts*, 2nd ed.; Wiley: Chichester, 1994.

(20) Huang, H. Y.; Yang, R. T. *Ind. Eng. Chem. Res.* **2003**, *42*, 2427.

(21) Cornelius, M.; Hoffmann, F.; Fröba, M. *Chem. Mater.* **2005**, *17*, 6674.

(22) Ou, L. D.; Seddon, A. B. *J. Non-Cryst Solids* **1997**, *210*, 187.

(23) (a) Hanoudi, Si.; Yang, Y.; Moudrakovski, I. L.; Lang, S.; Sayari, A. *J. Phys. Chem. B* **2001**, *105*, 9118. (b) Adima, A.; Moreau, J. J. E.; Wong Chi Man, M. *J. Mater. Chem.* **1997**, *7*, 2331. (c) Ek, S.; Iiskola, E. I.; Niinistö, L.; Vaitinen, J.; Pakkanen, T. T.; Root, A. *J. Phys. Chem. B* **2004**, *108*, 11454.

(24) Brethon, A.; Moreau, J. J. E.; Wong, Chi, Man, M. *Tetrahedron: Asym.* **2004**, *15*, 495.

(25) Guo, W. P.; Park, J. Y.; Oh, M. O.; Jeong, H. W.; Cho, W. J.; Kim, I.; Ha, C. S. *Chem. Mater.* **2003**, *15*, 2295.

(26) (a) Bellamy, L. J. *Infra-red Spectra of Complex Molecules*, 2nd ed.; Methuen: London, 1958. (b) Cross, A. D. *Introduction to Practical Infra-red Spectroscopy*; Butterworths Scientific Publications: London, 1960.

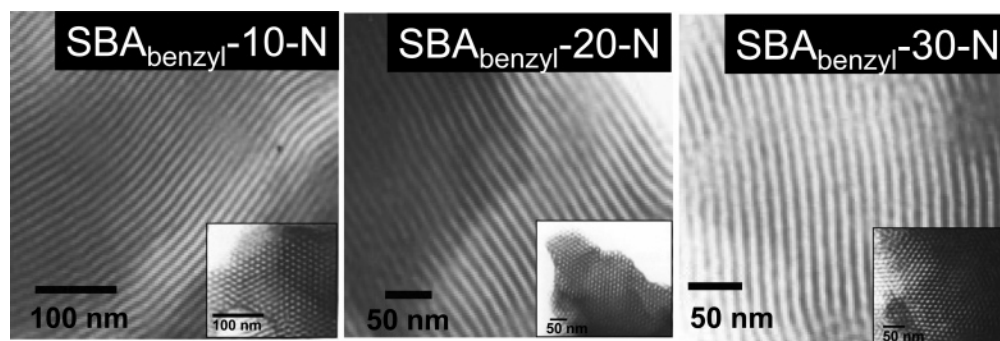


Figure 4. TEM images of $\text{SBA}_{\text{benzyl-}n\text{-N}}$ [n is the molar percent of $\text{M}_{\text{benzyl}}/(\text{M}_{\text{benzyl}} + \text{BTME})$]: viewed in the direction perpendicular to the pore axis and along the direction of the pore axis (inset).

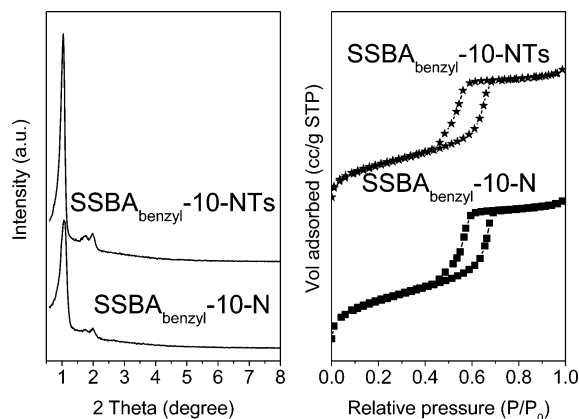


Figure 5. Powder XRD patterns and nitrogen adsorption-desorption isotherms of $\text{SSBA}_{\text{benzyl-}10\text{-N}}$ [10 is the molar percent of $\text{M}_{\text{benzyl}}/(\text{M}_{\text{benzyl}} + \text{TEOS})$] and $\text{SSBA}_{\text{benzyl-}10\text{-NTs}}$ [the material prepared by postmodification of $\text{SSBA}_{\text{benzyl-}10\text{-N}}$ with p -toluenesulfonyl chloride].

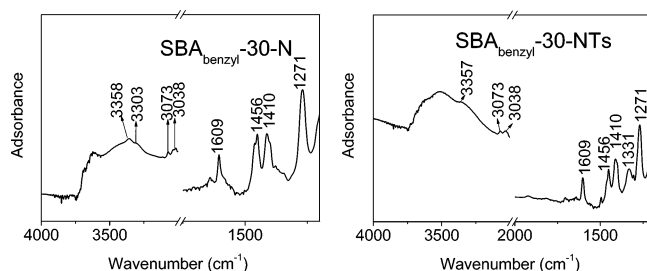


Figure 6. FT-IR spectra of $\text{SBA}_{\text{benzyl-}30\text{-N}}$ and $\text{SBA}_{\text{benzyl-}30\text{-NTs}}$ [30 is the molar percent of $\text{M}_{\text{benzyl}}/(\text{M}_{\text{benzyl}} + \text{BTME})$].

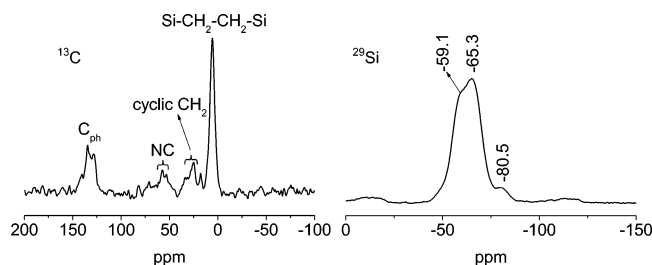


Figure 7. Solid-state ^{13}C CP-MAS NMR and ^{29}Si CP-MAS NMR spectra of $\text{SBA}_{\text{benzyl-}30\text{-N}}$ [30 is the molar percent of $\text{M}_{\text{benzyl}}/(\text{M}_{\text{benzyl}} + \text{BTME})$].

of sulfonamide group, is obviously noted due to the introduction of p -toluenesulfonyl group into $\text{SBA}_{\text{benzyl-}30\text{-NTs}}$.²⁶

The content of chiral moiety in the materials was calculated based on N elemental analysis (Table 2). From $\text{SBA}_{\text{benzyl-}0\text{-NRh}}$ to $\text{SBA}_{\text{benzyl-}30\text{-NRh}}$, the amount of chiral moiety is increased from 0 to 0.93 mmol/g, showing that a higher concentration of M_{benzyl} in the initial gel mixture could

Table 2. Asymmetric Transfer Hydrogenation of Acetophenone Using i -PrOH as H-Donor on $\text{SBA}_{\text{benzyl-}n\text{-NRh}}$ and $\text{SSBA}_{\text{benzyl-}10\text{-NRh}}$

| catalyst | chiral ligand ^a (mmol/g) | Rh (mmol/g) | Rh/chiral ligand | conv. ^b /% | ee/% (S) |
|---|--|----------------|---------------------|-----------------------|-------------|
| $\text{SBA}_{\text{benzyl-}10\text{-NRh}}$ | 0.30 (0.69) | 0.16 | 53 | 98 | 32 |
| $\text{SBA}_{\text{benzyl-}20\text{-NRh}}$ | 0.64 (1.29) | 0.19 | 30 | 94 | 33 |
| $\text{SBA}_{\text{benzyl-}30\text{-NRh}}$ | 0.93 (1.78) | 0.36 | 39 | 98 | 30 |
| $\text{SSBA}_{\text{benzyl-}10\text{-NRh}}$ | 0.61 (1.26) | 0.41 | 67 | 85 | 33 |
| $\text{M}_{\text{benzyl}}:\text{Rh}^c$ | | | | 93 | 36 |

^a The quantity of chiral ligand in the solids is calculated from elemental analyses. The values in the parentheses are the theoretical estimations of chiral ligand in the solids, which is calculated based on the formula $(\text{O}_{1.5}\text{SiCH}_2\text{CH}_2\text{SiO}_{1.5})_{100-n}(\text{RSiO}_{1.5})_n$ or $(\text{SiO}_2)_{100-n}(\text{RSiO}_{1.5})_n$, while R is the chiral ligand and $n = 10, 20, 30$. ^b $[\text{Rh}(\text{cod})\text{Cl}]_2$ as metal source. Conversion is based on acetophenone. Reaction conditions: catalysts (7.36 μmol of Rh), i -PrOH (12 mL), i -PrOK (0.1 mmol), acetophenone (2 mmol), reaction temperature ($83 \pm 2^\circ\text{C}$), reaction time (3 h). ^c Homogeneous catalyst: M_{benzyl} (2.4 mg, 7.36 μmol) was in situ coordinated with $[\text{Rh}(\text{cod})\text{Cl}]_2$ (1.8 mg, 3.68 μmol) in the solvent of i -PrOH (12 mL) at room temperature for 1 h. The catalytic reaction was performed under conditions identical to those of the heterogeneous catalysts.

result in the material with higher concentration of chiral moiety. Compared with the theoretical value, we know that about 43% of M_{benzyl} in the initial gel mixture could be effectively incorporated in the material. The Rh content of $\text{SBA}_{\text{benzyl-}n\text{-NRh}}$ increases with the content of the chiral moiety in the material, indicating that the chiral moieties in the mesopore are accessible to the guest molecules. However, the Rh content of $\text{SBA}_{\text{benzyl-}n\text{-NRh}}$ does not increase linearly with the amounts of chiral moiety in the material. Rh/chiral ligand ratio is 53% and 39% for $\text{SBA}_{\text{benzyl-}10\text{-NRh}}$ and $\text{SBA}_{\text{benzyl-}30\text{-NRh}}$, respectively. The above results show that some of the chiral moieties may be buried in the mesoporous framework or crowded in the channel, which could not be accessed by Rh complex.

3.3. Catalytic Properties of the Mesoporous Organosilicas for the Asymmetric Transfer Hydrogenation (ATH) of Ketones. The coordination of rhodium complex with trans -(1*R*,2*R*)-diaminocyclohexane in the catalysts was characterized by diffuse-reflectance UV-vis spectroscopy (Figure 8). $\text{SBA}_{\text{benzyl-}30\text{-N}}$ shows two sharp peaks in the range of 200–300 nm originating from the phenyl group and ethane group in the material. $[\text{Rh}(\text{cod})\text{Cl}]_2$ and $[\text{RhCp}^*\text{Cl}_2]_2$

Table 3. Asymmetric Transfer Hydrogenation of Acetophenone Using HCOONa as H-Donor on SBA_{benzyl}-30-NRhCp, SBA_{benzyl}-30-NTsRhCp, and SSBA_{benzyl}-10-NTsRhCp

| catalyst | chiral ligand (mmol/g) | Rh (mmol/g) | Rh/chiral ligand | conv. ^a /% | ee/% |
|------------------------------------|------------------------|-------------|------------------|-----------------------|--------|
| SBA _{benzyl} -30-NRhCp | 0.93 (1.78) | 0.46 | 49 | 18 | 38 (S) |
| SBA _{benzyl} -30-NTsRhCp | 0.93 (1.78) | 0.44 | 47 | 53 | 68 (R) |
| SSBA _{benzyl} -10-NTsRhCp | 0.61 (1.26) | 0.50 | 82 | 19 | 37 (R) |
| homogeneous catalyst ^b | | | | 62 | 65 (R) |

^a [RhCp*Cl₂]₂ as metal source. Conversion is based on acetophenone. Reaction conditions: catalysts (0.01 mmol of Rh), HCOONa (5 mmol), H₂O (2 mL), acetophenone (0.5 mmol), reaction temperature (40 °C), reaction time (10 h), air atmosphere. ^b Homogeneous ligand (3.6 mg, 0.01 mmol), [RhCp*Cl₂]₂ (3.1 mg, 0.005 mmol).

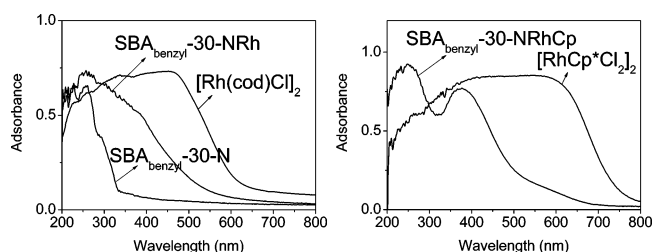
**Figure 8.** UV-vis spectra of Rh complexes (solid powder) and SBA_{benzyl}-30-N before and after complexing with Rh complexes.

exhibit an adsorption maximum at about 450 and 600 nm, respectively. After complexing with [Rh(cod)Cl]₂ or [RhCp*Cl₂]₂, SBA_{benzyl}-30-NRh or SBA_{benzyl}-30-NRhCp exhibits a new peak at about 380 nm, respectively. These findings confirm that the rhodium complex coordinated with *trans*-(1*R*,2*R*)-diaminocyclohexane in the materials.²⁴

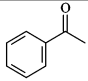
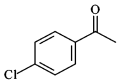
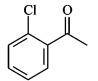
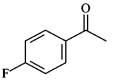
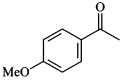
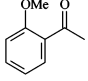
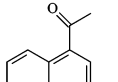
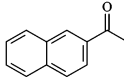
The ATH of acetophenone with *i*-PrOH as H-donor was carried out on SBA_{benzyl}-*n*-NRh (*n* = 10, 20, 30) and SSBA_{benzyl}-10-NRh. 2-Phenethylalcohol is the only product detected. All the catalysts are active for this reaction. SBA_{benzyl}-*n*-NRh (*n* = 10, 20, 30) with ethane moiety in the framework exhibits 94–98% conversion with 30–33% ee within 3 h, while the homogeneous catalyst (formed by complexing [Rh(cod)Cl]₂ with **M**_{benzyl}) gives 93% conversion of acetophenone with 36% ee under identical reaction conditions (Table 2). The catalytic activity and enantioselectivity of SBA_{benzyl}-*n*-NRh are comparable with those of the homogeneous catalyst. This result indicates that most (if not all) ligands retain their chirality on the mesoporous materials synthesized under acidic conditions. SSBA_{benzyl}-10-NRh with the pure-silica framework exhibits a lower conversion of 85% with 33% ee within 3 h. This result shows that the presence of ethane group in the framework can enhance the catalytic activity of the catalyst. This observation is consistent with our previous report.¹²

With use of *i*-PrOH as H-donor, the ATH of ketone is reversible, which deteriorates the enantioselectivity and prevents a complete conversion of ketone. In this regard, the HCOONa–H₂O system provides a good replacement

because it can react with ketone irreversibly. Moreover, catalysis in water is greener. We tried to use SBA_{benzyl}-30-NRhCp in the HCOONa–H₂O system. But the catalyst gives only a conversion of 18% with 38% ee (S) (Table 3). Recently, Xiao and co-workers reported that (1*R*,2*R*)-*N*-(*p*-toluenesulfonyl)-1,2-cyclohexanediamine-Rh can efficiently catalyze the ATH of aromatic ketones by HCOONa in water under air atmosphere.¹³ We also tried to use *p*-toluenesulfonyl chloride to modify the diamine in SBA_{benzyl}-*n*-N. For SBA_{benzyl}-*n*-N, *trans*-(1*R*,2*R*)-diaminocyclohexane was covalent-bonded to the material using benzyl group as linker, in which one NH₂ of diamine was reacted with benzyl chloride group and the other NH₂ is free. The free NH₂ of *trans*-(1*R*,2*R*)-diaminocyclohexane on the material provides an opportunity for further postmodification of DACH in the mesopore. In the HCOONa–H₂O system, SBA_{benzyl}-30-NTsRhCp, the modified catalyst, exhibits 53% conversion with 68% ee (R), which is much higher than SBA_{benzyl}-30-NRhCp's (Table 3). It is noteworthy to mention that the configuration of the product catalyzed by the modified catalyst is opposite that catalyzed by the unmodified catalyst, which further confirms the successful postmodification of DACH in the mesopore. The activity and enantioselectivity of SBA_{benzyl}-30-NTsRhCp are comparable to those of the corresponding homogeneous catalyst [62% conversion with 65% ee (R)]. SSBA_{benzyl}-10-NTsRhCp shows a lower conversion of 19% with 37% ee (R) than SBA_{benzyl}-30-NTsRhCp, again indicating that the existence of ethane group in the framework of the material enhances the catalytic activity of the catalyst.¹²

Moreover, a number of different aromatic ketones can be converted into the corresponding chiral alcohol on SBA_{benzyl}-30-NTsRhCp (Table 4). The structures and electronic properties of the ketones significantly affect the catalytic performance of SBA_{benzyl}-30-NTsRhCp. Acetophenones bearing substituents in the para position result in higher enantioselectivity than those in the ortho position (entries 2, 5 vs entries 3, 6). More crowded 1- or 2-acetylnaphthalene is also converted into the corresponding alcohols. 2-Acetylnaph-

Table 4. Asymmetric Transfer Hydrogenation of Aromatic Ketones Using HCOONa as H-Donor on SBA_{benzyl}-30-NTsRhCp

| Entry | Substrate | Conv. ^a /% | ee/% (R) |
|-------|---|-----------------------|----------|
| 1 |  | 53 | 68 |
| 2 |  | 54 | 74 |
| 3 |  | 58 | 45 |
| 4 |  | 53 | 70 |
| 5 |  | 16 | 39 |
| 6 |  | 25 | 18 |
| 7 |  | 12 | 47 |
| 8 |  | 33 | 81 |

^a [RhCp*Cl₂]₂ as metal source. Conversion is based on ketones. Reaction conditions: catalysts (0.01 mmol of Rh), HCOONa (5 mmol), H₂O (2 mL), acetophenone (0.5 mmol), reaction temperature (40 °C), reaction time (10 h), air atmosphere.

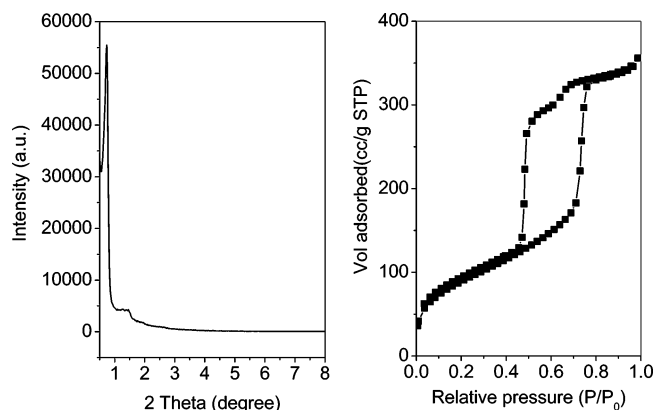
Table 5. Recycle Studies of SBA_{benzyl}-30-NTsRhCp for the Asymmetric Transfer Hydrogenation of Acetophenone with HCOONa as H-Donor in H₂O

| catalyst | no. of recycles | conv. ^a /% | ee/% |
|---|-----------------|-----------------------|--------|
| SBA _{benzyl} -30-NTsRhCp | 0 | 53 | 68 (R) |
| | 1 | 33 | 66 (R) |
| | 1 ^b | 33 | 53 (R) |
| | 2 | 10 | 65 (R) |
| [RhCp*Cl ₂] ₂ ^c | | 7 | 0 |

^a [RhCp*Cl₂] as metal source. Conversion is based on acetophenone. Reaction conditions: catalysts (0.01 mmol of Rh), HCOONa (5 mmol), H₂O (2 mL), acetophenone (0.5 mmol), reaction temperature (40 °C), reaction time (10 h), air atmosphere. ^b [RhCp*Cl₂]₂ was added to the reaction system during the first recycle. The amount of the added metal complex was based on the assumption that no Rh complex remains on the reused catalyst. ^c The reaction was carried out using only [RhCp*Cl₂]₂ as catalyst.

thalene (entry 8) shows 33% conversion with 81% ee, while 12% conversion with 47% ee is observed on 1-acetylnaphthalene (entry 7). These observations are consistent with those from the literature.^{27,28}

The reusability of SBA_{benzyl}-30-NTsRhCp was tested for the asymmetric transfer hydrogenation of acetophenone

**Figure 9.** Powder XRD patterns and nitrogen adsorption–desorption isotherms of the used SBA_{benzyl}-30-NTsRhCp after the first reaction cycle.

(Table 5). The catalytic activity of the reused catalyst is decreased to 33% after the first cycle. For the second cycle, the catalytic activity is only 10%. The ee value remains almost the same during the recycle (68–65%). After the first reaction, the used SBA_{benzyl}-30-NTsRh still has well-ordered mesostructure with BET surface area of about 300 m²/g, similar to that of the refresh catalyst (Figure 9). So the deactivation of the catalyst is not due to the deterioration of the catalyst's structure. It was calculated that 23% of rhodium was leached from the catalyst after the first reaction. Therefore, the leaching of Rh metal might be one of the main reasons for the decreasing of catalytic activity. Further addition of [RhCp*Cl₂]₂ into the catalytic system could not regain the activity and enantioselectivity, which showed that decomposition or deactivation of the active species would occur irreversibly in the reaction.^{28,29}

4. Conclusions

Large-pore mesoporous ethane-silicas functionalized with *trans*-(1*R*,2*R*)-diaminocyclohexane was synthesized for the first time under an acidic medium using P123 as template. The content of chiral moiety in the ordered mesoporous material can reach as high as 0.93 mmol/g. The presence of ethane group in the framework can enhance the catalytic activity of the resulting catalysts for the asymmetric transfer hydrogenation (ATH) of acetophenone. The mesoporous ethane-silica with new chiral moiety generated by the postmodification method exhibits significantly improved activity and enantioselectivity for the ATH of acetophenone in the HCOONa–H₂O system under air atmosphere. The present synthesis strategy, direct synthesis associated with postmodification, is a facile method to synthesize mesoporous materials with a new chiral functional group.

Acknowledgment. Financial support of this work was provided by the National Natural Science Foundation of China (20303020, 20321303) and National Basic Research Program of China (2003CB615803).

CM0613307

(27) (a) Li, X. G.; Wu, X. F.; Chen, W. P.; Hancock, F. E.; King, F.; Xiao, J. L. *Org. Lett.* **2004**, 6, 3321. (b) Wu, X. F.; Li, X. G.; Hems, W.; King, F.; Xiao, J. L. *Org. Biomol. Chem.* **2004**, 2, 1818.

(28) Li, X. G.; Chen, W. P.; Hems, W.; King, F.; Xiao, J. L. *Tetrahedron Lett.* **2004**, 45, 951.

(29) Liu, P. N.; Gu, P. M.; Wang, F.; Tu, Y. Q. *Org. Lett.* **2004**, 6, 169.